Cation Complexation by Chemically Modified Calixarenes. 11. Complexation and Extraction of Alkali Cations by Calix[5]- and -[6]arene Ketones. Crystal and Molecular Structures of Calix[5]arene Ketones and Na^+ and Rb^+ Complexes

Steven E. J. Bell, Julie K. Browne, Vickie McKee, M. Anthony McKervey,* John F. Malone, Maeve O'Leary, and Andrew Walker

School of Chemistry, The Queen's University, Belfast BT9 5AG, N. Ireland

Francoise Arnaud-Neu, Olivier Boulangeot, Olivier Mauprivez, and Marie-Jose Schwing-Weill

Laboratoire de Chimie-Physique, URA au CNRS 405, ECPM, 1, rue Blaise Pascal, 67000 Strasbourg, France

Received July 17, 1997[⊗]

A series of four calix[5]arenes and three calix[6]arenes (R-calixarene-OCH_2COR^1) (R = H or Bu^t) with alkyl ketone residues (R^1 = Me or Bu^t) on the lower rim have been synthesized, and their affinity for complexation of alkali cations has been assessed through phase-transfer experiments and stability constant measurements. The conformations of these ketones have been probed by ^{1}H NMR and X-ray diffraction analysis, and by molecular mechanics calculations. Pentamer **3** (R = R^1 = Bu^t) possesses a symmetrical cone conformation in solution and a very distorted cone conformation in the solid state. Pentamer **5** (R = H, R^1 = Bu^t) exists in a distorted 1,2-alternate conformation in the solid state, but in solution two slowly interconverting conformations, one a cone and the other presumed to be 1,2-alternate, can be detected. X-ray structure analysis of the sodium and rubidium perchlorate complexes of **3** reveal the cations deeply encapsulated by the ethereal and carbonyl oxygen atoms in distorted cone conformations which can be accurately reproduced by molecular mechanics calculations. The phase-transfer and stability constant data reveal that the extent of complexation depends on calixarene size and the nature of the alkyl residues adjacent to the ketonic carbonyls with *tert*-butyl much more efficacious than methyl.

The ability of carbonyl-containing substituents on the lower rim of calixarenes[1] to act as ligating podands for encapsulation of metal and ammonium cations is now well established.[2−4] The majority of studies describe the use of ester,[5−8] amide,[9,10] and carboxylic acid derivatives.[11] Apart from one published study[5,12] the use of ketonic carbonyl groups as potential binding sites on the calixarene substructure is unexplored, despite the greater donicity of ketones as compared with esters. We have conducted a systematic study of the behavior of ketones in the pentamer and hexamer series in complexation and extraction of alkali cations.

The pentamers are particularly attractive members of the calixarene homology, though they are the least studied. They possess larger peripheries than their calix[4]arene counterparts, and are presumably more mobile, yet retain the capability to adopt true cone conformations of C_{5v} symmetry. And although pentamers have not yet received the same degree of scrutiny regarding their conformational characteristics, some important features are beginning to emerge. Gutsche and co-workers[13] have recently completed a comprehensive study of a whole series of *p-tert*-butylcalix[5]arene ethers and esters, the results of which reveal that even though calix[5]arenes resemble tetramers in having four up/down conformations (cone, partial cone, 1,2-alternate, 1,3-alternate), there are many more opportunities for conformational subtleties associated with the degree of tilt of the individual aryl subunits within each of these four conformational categories. Furthermore, the NMR method alone may no longer provide a definitive distinction between the noncone conformations.

Synthesis of Calixarene Ketones

The compounds chosen for study were *p-tert*-butylcalix[5]arene pentamethyl ketone **1** and its calix[6]arene

[⊗] Abstract published in *Advance ACS Abstracts,* December 1, 1997.

(1) Gutsche, C. D. Calixarenes. In *Monographs in Supramolecular Chemistry*; Stoddart, J. F., Ed.; Royal Society of Chemistry: London, 1989; Vol. 1.

(2) Schwing-Weill, M.-J.; McKervey, M. A. In *Calixarenes, a Versatile Class of Macrocyclic Compounds*; Vicens, J., Bohmer, V., Eds.; Kluwer Academic Publishers: Dordrecht, 1990; pp 149−172.

(3) Schwing-Weill, M.-J.; Arnaud-Neu, F.; McKervey, M. A. *J. Phys. Org. Chem.* **1992**, *5*, 496.

(4) Ungaro, R.; Pochini, A. Reference 2, pp 127−147.

(5) Arnaud-Neu, F.; Collins, E. M.; Deasy, M.; Ferguson, G.; Harris, S. J.; Kaitner, B.; Lough, A. J.; McKervey, M. A.; Marques, E.; Ruhl, B. L.; Schwing-Weill, M.-J.; Seward, E. M. *J. Am. Chem. Soc.* **1989**, *111*, 8681.

(6) Chang, S. K.; Cho, I. *J. Chem. Soc., Perkin Trans. 1* **1986**, 211.

(7) Arduini, A.; Pochini, A.; Reverberi, S.; Ungaro, R.; Andreetti, G. D.; Ugozzoli, F.; *Tetrahedron* **1986**, *42*, 2089.

(8) Danil de Namor, A. F.; Gil, E.; Losa Tanco, M. A.; Pacheco Tanaka, D. A.; Pulcha Salazar, L. E.; Schulz, R. A.; Wang, J. *J. Phys. Chem.* **1995**, *99*, 16776.

(9) Arduini, A.; Pochini, A.; Reverberi, S.; Ungaro, R.; Andreetti, G. D.; Ugozzoli, F. *J. Incl. Phenom.* **1988**, *6*, 119.

(10) Arnaud-Neu, F.; Schwing-Weill, M.-J.; Ziat, K.; Cremin, S.; Harris, S. J.; McKervey, M. A. *New. J. Chem.* **1991**, *15*, 33.

(11) Arnaud-Neu, F; Barrett, G.; Harris, S. J.; McKervey, M. A.; Owens, M.; Schwing-Weill, M. J.; P. Schwinte. *Inorg. Chem.* **1993**, *32*, 2644.

(12) Ferguson, G.; Kaitner, B.; McKervey, M. A.; Seward, E. M. *J. Chem. Soc., Chem. Commun.* **1987**, 584.

(13) Stewart, D. R.; Krawiec, M.; Kashyap, R. P.; Watson, W. H.; Gutsche, C. D. *J. Am. Chem. Soc.* **1995**, *117*, 586.

S0022-3263(97)01311-X CCC: $15.00
Published on Web 01/16/1998

Scheme 1

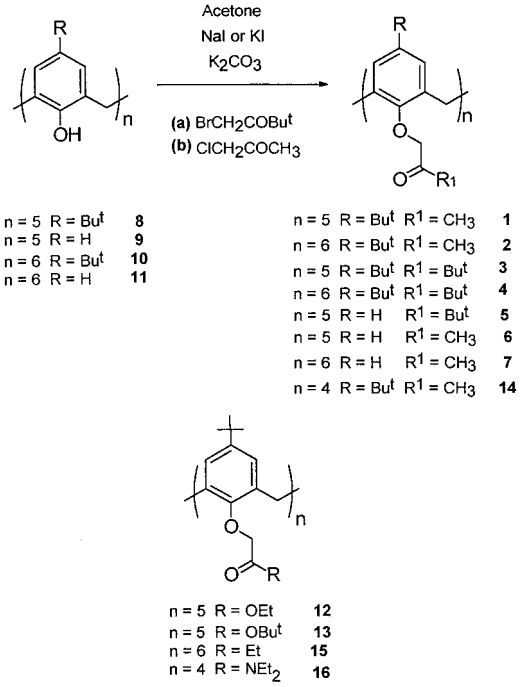

counterpart **2**; *p-tert*-butylcalix[5]arene penta *tert*-butyl ketone **3** and its hexamer counterpart **4**; calix[5]arene penta *tert*-butyl ketone **5**, calix[5]arene pentamethyl ketone **6**, and calix[6]arene hexamethyl ketone **7**.

All six compounds were prepared from the appropriate calixarene (**8**−**11**) by exhaustive alkylation with either chloroacetone or bromopinacolone (Scheme 1) in dry acetone containing potassium carbonate and potassium or sodium iodide, the latter to activate the electrophile through halogen exchange. In the case of pentaketones **3** and **5** with pinacolone moieties on the lower rim, the products were isolated as K^+ complexes. Decomplexation of **5** was accomplished by treatment with water at 60 °C; prolonged treatment with aqueous ethanol (3 days under reflux) was required to release ketone **3** from its complex. Analytically pure samples of all six ketones were obtained by recrystallization from ethanol-dichloromethane. ^{1}H NMR analysis provided some insight into the conformations of these ketones and their complexes in solution. The crystal and molecular structures of **1**, **3**, and **5** and of the sodium and rubidium perchlorate complexes of **3** have been determined by X-ray diffraction and compared with structures simulated by molecular mechanics.

Conformation of Calixarene Ketones

In our earlier work on calix[5]arene acetates of type **12** and **13** we found evidence in solution for the presence of stable cone conformations of presumed averaged C_{5v} symmetry.[14] X-ray diffraction confirmed the cone conformation in the solid state for **12**, but further revealed a distortion of the cone which does not approximate to any regular geometric arrangement. One of the five aryl rings tilts inward so that its *tert*-butyl group overhangs the cavity on the upper rim, while the remaining four tilt outward, as is normal, but to different extents. Penta

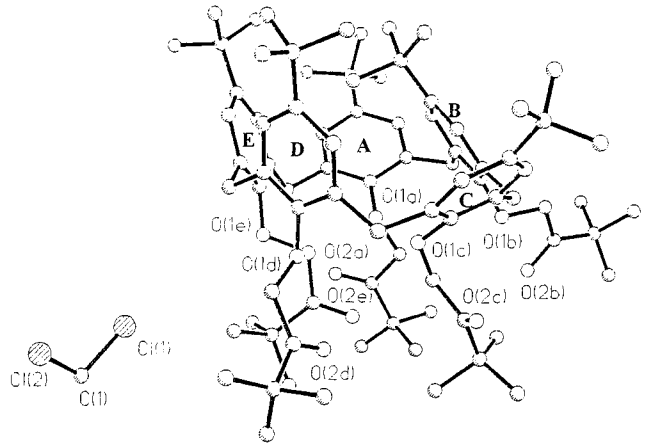

Figure 1. A view of molecule **3** showing the molecular conformation.

tert-butyl ketone **3** shares these features to a considerable degree. The aromatic, methyleneoxy and both *tert*-butyl group protons in the ^{1}H NMR spectrum appear as singlets with an AB pattern for the bridging methylene groups, suggesting a symmetrical cone conformation. Solid-state IR analysis, however, revealed two carbonyl absorptions of unequal intensity at 1699 and 1729 cm^{-1}, indicative of a less symmetrical arrangement with the implication that the symmetrical solution state structure is the result of a rapid conformation averaging process. X-ray diffraction (Figure 1) revealed that the molecule does possess a cone conformation in the solid state and with the same type of distortion as that found in its pentaester counterpart **12**.[14] The spatial void in the upper rim cavity is partially occupied by inclination of one *tert*-butyl group. The conformation of **3** is best described by the angles that the aromatic rings (A−E) make with the mean plane of the five macrocyclic ring methylene groups, viz.: (137°: A), (56°: B), (140°: C), (101°: D) and (107°: E). An angle greater than 90° implies the aromatic ring is tilted in a manner that pitches its attached *tert*-butyl group away from the calix cavity while for angles less than 90° the reverse is true. Inspection of these tilting angles reveals that while ring B tilts in markedly, the remaining aromatic rings are inclined outward but by very different amounts. The inward disposition of ring B necessarily forces adjoining rings A and C to adopt a more open arrangement in relation to the remaining macrocyclic aromatic units. This effect is reflected in the tilting angles of rings A (137°) and C (140°) where the greater outward tilt compared to rings D (101°) and E (107°) reduces steric interaction between the *tert*-butyl groups on rings A and C with that on ring B. This structural distortion may also relieve the conformational strain imposed on the adjacent bridging methylene carbon atoms by the inclination of ring B. The inter-ring methylene carbons deviate considerably from coplanarity as a result of distortion with individual atoms as much as 0.43 Å from the mean plane.

The pendent ketone side chains adopt very different spatial arrangements. Ketone chains A, C, D and E take up positions below the calix cage with ketone arm E filling the lower rim cavity in much the same way as has been observed with the pentaethyl ester. The inward inclination of aryl ring B forces its attached ketone arm to be directed away from the calix cage. The uncom-

(14) Barrett, G.; McKervey, M. A.; Malone, J. F.; Walker, A.; Arnaud-Neu, F.; Guerra, L.; Schwing-Weill, M.-J.; Gutsche, C. D.; Stewart, D. R. *J. Chem. Soc., Perkin Trans. 2* **1993**, 1475.

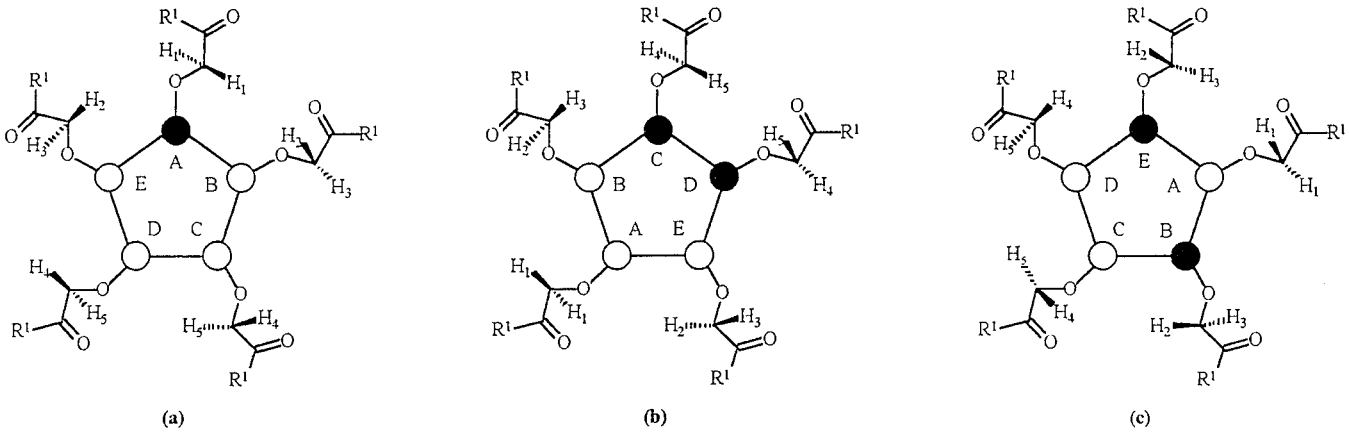

Figure 2. Iconographic representation and NMR symmetry patterns for noncone conformations of *p-tert*-butylcalix[5]arene ketones.

plexed pentaketone cavity is thus enclosed by a distorted pentagonal pyramid composed of the five phenolic oxygen atoms (O1A−O1E) and the carbonyl oxygen atom (O2E). The remaining carbonyl oxygen atoms take up random positions around the lower rim calix cage. Adjacent phenolic O--O separations around the lower rim vary between 3.30 Å (O1C−O1D) and 4.51 Å (O1B−O1C) highlighting the outward disposition of chain B. A molecule of methylene chloride is present within the crystal lattice, but there are no short intermolecular contacts to the calixarene. Some of the *tert*-butyl groups of **3** were disordered with high thermal parameters and where appropriate were restrained using the computational features (SAME, SADI) available in SHELXL 93.[15]

Changing the alkyl residue adjacent to the carbonyl group in ketone **3** from *tert*-butyl to methyl as in **1** has a profound effect on the conformations adopted in the pentamer series. The ^{1}H NMR spectrum of **1** at room temperature consists of a series of broad, partly resolved signals indicative of rapid fluxional behavior. It is probable that conformational interconversion in **1** proceeds via the oxygen through the annulus pathway where the ketonic methyl chains are sufficiently small to pass through the cavity of the pentamer, unlike the sterically more consuming ketonic *tert*-butyl chains in nonfluxional **3**. At low temperatures in solution (−10 °C) this fast fluxional motion in **1** is suppressed and a series of well-resolved ^{1}H NMR resonances result, from which a conformational assignment was tentatively made. The ^{1}H NMR spectrum of **1**, at −10 °C, shows five sets of aryl H resonances in a 1:1:1:1:1 ratio of two doublets (7.10, J = 1.8 Hz, 7.13 ppm, J = 1.1 Hz) and three singlets (7.19, 7.37, and 7.58 ppm), illustrating immediately that **1** does not adopt the same symmetrical cone arrangement that was observed for **3**. The $ArCH_2Ar$ bridging methylene region is very complex, a problem compounded by the fact that the OCH_2 ketonic group protons also appear in this area. To make an assignment it was assumed that the OCH_2 protons would overlap only with the more downfield H_A signals of the $ArCH_2Ar$ methylene protons and would not interfere with the much more shielded, upfield, H_B of the $ArCH_2Ar$ methylene hydrogens. By employing a series of decoupling experiments and a 2D ^{1}H COSY NMR spectrum of **1**, it was possible to assign H_B protons coupled to their methylene H_A counterparts, a process ultimately verified by the close similarity of the coupling constants of the assigned partners. On this basis the $ArCH_2Ar$ protons appear as three pairs of doublets at 3.29 (2H, H_B), 3.34 (1H, $H_{B'}$), 3.81 (2H, $H_{B''}$), 4.01 (2H, $H_{A''}$), 4.13 (1H, $H_{A'}$), and 4.21 (2H, H_A) ppm. Such a spectral pattern is commensurate with a partial cone, a 1,2-alternate or a 1,3-alternate conformational orientation. The OCH_2 protons show an unusual arrangement in this ketone producing two singlet resonances at 4.17 and 4.22 ppm and one pair of doublet resonances at 4.16 and 4.53 ppm in a 1:2:2 ratio, respectively. This implies that the rigidifying process accompanying conformational freezing is accentuating the nonequivalent nature of some of these protons which are illustrated iconographically in Figures 2a−c for the partial cone, 1,2-alternate, and 1,3-alternate conformers, respectively. The environment of the OCH_2 protons in **1** is such that four of the nonequivalent hydrogen atoms appear as a singlet at 4.22 ppm rather than a pair of doublets which might have been expected on the basis of the symmetry arguments shown in Figure 2. This suggests that these four protons are in chemically similar environments which is tentatively possible for ketone arms D and C in Figure 2a and ketone arms B and E in Figure 2c but not for ketone chains C, D or B, E in Figure 2b. This implies, therefore, that **1** may assume a partial cone arrangement (Figure 2a), or a 1,3-alternate orientation (Figure 2c), in solution. The *tert*-butyl protons appear as three singlets at 1.15, 1.33, and 1.44 ppm in a 2:2:1 ratio, a pattern reminiscent of a partial cone, 1,2-, or 1,3-alternate species. The terminal methyl groups on the ketone chains also appear as three singlets at 0.75, 1.00−1.09 (broadened), and 2.11 ppm in a 1:2:2 ratio. One methyl group occupies the most shielded position at 0.75 ppm, a feature indicative of a partial cone conformer. However, a partial cone conformer would be expected to contain the remaining four methyl groups in fairly similar environments which should be reflected in relatively closely separated chemical shift positions. This is not the case for **1**, in which the other four CH_3 protons are widely separated, two sets being deshielded at 2.11 ppm and the remaining two much more shielded at 1.00−1.09 ppm. This spectral arrangement is much more consistent with a 1,2- or 1,3-alternate conformation. The ^{13}C NMR spectrum (−10 °C) of **1** displays two downfield $ArCH_2Ar$ resonances between the at 34.08 and 34.22 ppm for the methylene carbons between the *anti*-aryl rings and only one upfield $ArCH_2$-Ar signal at 31.39 ppm for the *syn*-aryl rings, a pattern consistent only with a 1,3-alternate conformation. On

(15) Sheldrick, G. M. University of Göttingen, 1993. SHELXL 93.

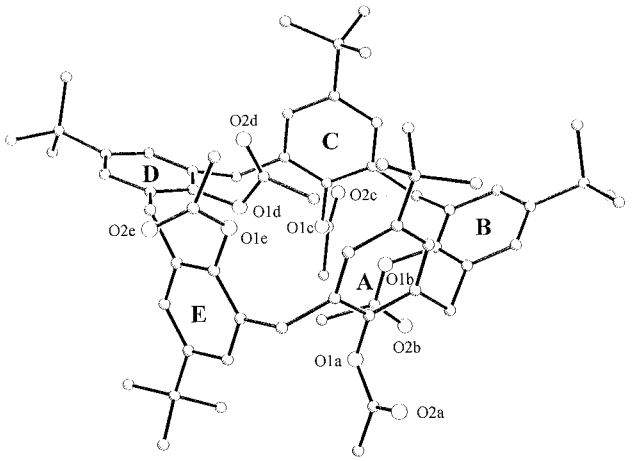

Figure 3. A view of molecule **1** showing the molecular conformation.

the basis of these spectral observations, the 1,3-alternate isomer is deemed most probable for compound **1**. Solid-state IR spectroscopic analysis of **1** shows two carbonyl absorptions at 1715 and 1738 cm^{-1} indicative of a structural form which places the carbonyl oxygens in nonidentical environments in accord with the solution state structure. In contrast to our analysis of the solution conformation of ketone **1** we found by X-ray diffraction that in the solid state the arrangement is that of a very distorted 1,2-alternate conformation (Figure 3). The asymmetric unit comprises the calixarene and one molecule of dichloromethane solvate; there is no evidence of any interaction between calixarene and solvate. The calixarene conformation is irregular and can be described in terms of the tilt angles of the phenyl rings to the plane of the five macrocyclic methylene groups: (92°: A, 141°: B, 87°: C, 7°: D and 86°: E). Rings A, C, and E are almost perpendicular to the cavity, B is tilted with the *tert*-butyl group outward and D almost coplanar with the plane of the five methylene groups. Ring E is inverted so that its *tert*-butyl group lies on the opposite rim to those of rings A, B, and C.

Ketone **6** is also a methyl derivative of a calix[5]arene but lacks a *p-tert*-butyl substituent. The ^{1}H NMR spectrum of **6** shows that this molecule is also fluxional at room temperature. Aryl rotation in **6** can be accomplished by an oxygen through the annulus pathway or a *para* hydrogen through the annulus pathway. The former is supported by the behavior of **1**, where it is known that rotation of the *para* substituent through the calix is precluded. Nevertheless, the molecule is fluxional. At −10 °C the conformational mobility of ketone **6** is suppressed and the ^{1}H NMR spectrum now appears as a series of sharp signals whose multiplicity is inconsistent with a cone conformation. The calix aromatic protons appear as a series of coupled signals at 6.77−7.57 ppm providing little information concerning the precise conformation of **6**. Again, an assumption, similar to that made for ketone **1**, was employed, regarding the assignment of the $ArCH_2Ar$ methylene region. The H_B $ArCH_2Ar$ protons in **6** were thus judged to be the most shielded hydrogens in this region. With the combination of a series of decoupling experiments and a 2D ^{1}H COSY NMR analysis, the corresponding H_A coupling partners could be identified. On this basis the $ArCH_2Ar$ protons again appear as three pairs of doublets, verifiable by corresponding coupling constants, at 3.33 (2H, H_B), 3.40 (1H, $H_{B'}$), 3.79 (2H, $H_{B''}$), 3.98 (2H, $H_{A''}$), and 4.12 ppm (1H, $H_{A'}$ and 2H, H_A overlapping). This spectral arrangement is consistent with a partial cone, 1,2-, or 1,3-alternate conformation. The OCH_2 protons appear as a singlet (4.23 ppm), a pair of doublets (4.20 and 4.53 ppm), and a multiplet (4.04 ppm exhibiting AB coupling) in a 1:2:2 ratio, respectively. Such a pattern is more consistent with a partial cone or 1,3-alternate arrangement (see Figure 2) where two sets of OCH_2 protons lie in chemically similar environments. The terminal methyl groups of the ketone chains appear as three singlets at 0.56, 1.43 (broadened), and 2.14 ppm in a 1:2:2 ratio, respectively. The extreme upfield position (0.56 ppm) of just one methyl group is consistent with a partial cone conformation. This observation is supported by the −10 °C ^{13}C NMR spectrum of **6** which reveals just one downfield resonance at 36.71 ppm indicative of aligned *anti* aromatic rings and two upfield resonances at 26.95 and 28.82 ppm indicative of *syn* aromatic rings, suggesting a partial cone or a 1,2-alternate conformer. Taking all the spectral data into account, a partial cone isomer is chosen as the most likely conformation. Solid-state IR spectroscopic analysis of **6** revealed two carbonyl stretches at 1723 and 1744 cm^{-1} in accord with the solution state structure.

Ketone **5**, the *para*-hydrogen analogue of **3**, was first isolated as a K^+ complex (*vide supra*). The ^{1}H NMR spectrum of the complex clearly pointed to the presence of a symmetrical cone conformation in solution. In contrast, the spectrum of **5** in the uncomplexed state at room temperature consisted of a complicated series of sharp signals attributable to the presence of two fixed (on the NMR time scale) conformations, a cone (17%) and a noncone (83%). However, the isolation of one K^+ complex indicated that conformational interconversion was possible, though at a rate sufficiently slow on the NMR time scale to distinguish two conformational isomers. ^{1}H NMR measurements at higher temperatures did reveal the onset of coalescence of the signals representing the two conformations. This conformational isomerism in **5** raises the question as to the nature of the molecular motion responsible: a lower rim through the annulus motion, as is the case with calix[4]arene conformers, or an upper rim through the annulus motion? Although the latter is not observed with calix[4]arenes, even with *para* substituents as small as hydrogen, it has been observed with calix[6]arenes, not just with *para*-hydrogen substituents but also with *para-tert*-butyl substituents. Gutsche's view from inspection of molecular models that calix[5]arenes may fall between these two situations is supported by the behavior of pentaketones **3** and **5**. Thus, at normal temperatures calix[5]arenes with *p-tert*-butyl groups can only interconvert, if at all (cf **3**), via the lower rim motion through the annulus. With **5**, in contrast, the bulky *tert*-butyl substituent on the lower rim will surely inhibit this motion, but since slow interconversion does occur we can conclude that it does so by rotation of the upper rim *para*-hydrogen substituent through the annulus.

The major conformational isomer of **5** displayed a very complex arrangement of sharp signals with three *tert*-butyl singlets (ratio 2:2:1) and a series of doublets and multiplets which could be accommodated by either a 1,2-alternate, a 1,3-alternate, or a partial cone conformation without offering any compelling choice among the three. The minor isomer of **5** was readily identified as cone from

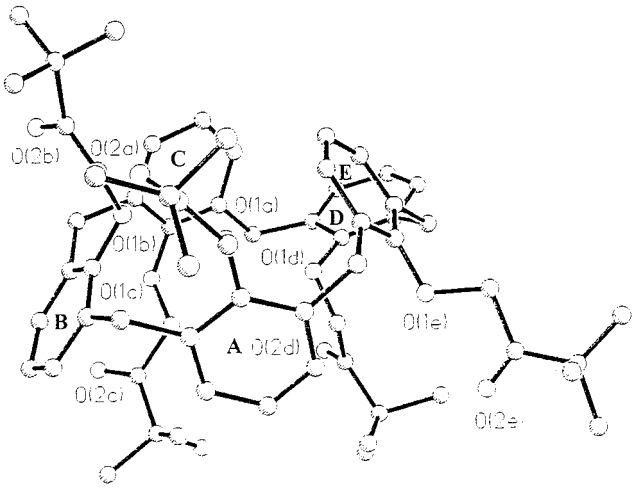

Figure 4. A view of molecule **5** showing the molecular conformation.

the ^{1}H NMR pattern. However, when crystalline **5** was analyzed by X-ray diffraction, only one conformation, the 1,2-alternate, was found in the solid state. But interestingly, when crystals of **5** were dissolved in $CDCl_3$, the ^{1}H NMR spectrum again revealed the presence of both cone and (presumed) 1,2-alternate conformations in a 83:17 ratio, confirming that interconversion does occur, leading eventually, in the presence of K^+ ion, to a cone complex. The structure adopted in the solid state by **5** is shown in Figures 4 and 5a. The compound assumes a very distorted 1,2-alternate orientation, implying that crystallization induces formation of this isomeric form preferentially. Two of the aromatic rings (groups A and D) in Figure 4 lies in a flattened orientation in comparison to the relatively less tilted arrangements of the remainder. Such extreme distortion from the more conventional up/down arrangement of aryl rings is reflected in the angular tilt of each aromatic unit from the macrocyclic methylene mean plane, viz.: (76°: A), (122°: B), (73°: C), (155°: D) and (56°: E). An angle of <90° implies that the aromatic *para* proton on each ring is directed into the calix cavity defined by the macrocyclic rim in question. An angle of >90° reflects the reverse situation. It must be noted, though, that the five bridging methylene groups in a noncone structure such as this are not coplanar, and significant deviations from the mean plane (as much as 0.66 Å) are prevalent. Nevertheless, the tilting angles provide a useful assessment of the distorted nature of this conformation. The structure as a whole provides a visual representation of the cavity size in relation to the podands.

Since the conformation of the major conformer of ketone **5** could not be unequivocally distinguished between a partial cone, a 1,2- or a 1,3-alternate isomer, it is probable that the solution state mirrors the solid state, and on this basis a 1,2-alternate arrangement is also likely to be adopted preferentially in solution. The remaining ketones, hexamers **2** and **7**, were conformationally mobile at room temperature.

Complexation Studies. Discussion

Physicochemical measurements of the efficacy of all seven ketones in complexation of alkali metal cations were conducted using biphase extraction of picrates from water into dichloromethane and stability constant determinations in methanol. Unfortunately, the latter, which provide a more precise expression of the thermodynamics of the complexation process, could not be extended to all ketones because of solubility limitations. Preliminary extraction experiments revealed a very large kinetic effect in the behavior of the *tert*-butyl ketone **3**. Whereas all the other ketones reached extraction equilibrium within minutes, it was necessary to allow several hours with **3** before reaching reproducible extraction levels. The data are summarized in Tables **1** and **2** which also contain for comparison the published data for pentaesters **12** and **13**, tetramethyl ketone **14**, and hexaester **15**. These data, illustrated graphically in Figures 6 and 7, reveal dramatic effects of calix size and substitution. The most striking aspect of the extraction data for alkali cations is the strong dependency on the nature of the alkyl residues adjacent to the ketonic carbonyls on the lower rim in the pentamer derivatives and, to a lesser extent, on the nature of the *para* substituent on the upper rim. The combination of *tert*-butyl substituents on *both* rims of the calixarene as in **3** produces the highest extraction levels for all alkali cations with, however, little discrimination between them after Li^+. The levels of extraction approach those observed earlier with tetraamides[10] and pentaamides.[22] Of the two, *tert*-butyl substitution on the lower rim appears to be the dominant influence. Thus, while replacing the *para tert*-butyl groups by hydrogen substituents as in **5** has the effect of reducing the overall extraction levels, e.g. Li^+ down from 58.4 to 8.3%, with leveling off for the larger cations now commencing at K^+, replacing the lower rim *tert*-butyl groups with methyl groups as in **1** has a much greater effect, reducing the extraction levels to a maximum of 11% (for Rb^+). The combination of *para*-hydrogen substituents on the upper rim and methyl substituents on the lower rim in **6** leads to the lowest levels of extraction in the entire pentaketone series. This contrasts with the effect of methyl ketones in the tetramer series, cf. compound **14**, where there is a strong sodium peak selectivity (42.3%). The reasons for the poor extraction performance of compounds **1** and **6** may lie in their conformational mobility and their inherent lack of any elements of preorganization. Tetraketone **14**, in contrast, is already in a fixed cone conformation prior to complexation. In the hexamer series ketonic binding groups are uniformly very inefficient with very low levels of alkali extraction for compounds **2**, **4**, and **7**.

For stability constants in methanol, the log β values (Table 2) for **5** reflect the trends in extraction with the higher values (5.67−5.84) associated with the larger cations. Unfortunately, comparative data for the double *tert*-butyl combination in **3** could not be obtained due to solubility limitations in methanol. Nevertheless, the beneficial effects of lower rim *tert*-butyl groups are again

(16) Guilbaud, P.; Varnek, A.; Wipff, G. *J. Am. Chem. Soc.* **1993**, *115*, 8298. Varnek, A.; Wipff, G. *J. Phys. Chem.* **1993**, *97*, 10840.
(17) Grootenhuis, P. D. J.; Kallman, P. A.; Groenen, L. C.; Reinhoudt, D. N.; van Hummel, G. J.; Ugozzoli, F.; Andreetti, G. D. *J. Am. Chem. Soc.* **1990**, *112*, 4165−4176.
(18) Stewart, D. R.; Gutsche, C. D. *Org. Prep. Proc. Intl.* **1993**, *25*, 137.
(19) Gutsche, C. D.; Iqbal, M. *Org. Synth.* **1990**, *68*, 234.
(20) Pedersen, C. J. *Fed. Proc. Fed. Am. Soc. Expl. Biol.* **1968**, *27*, 1305.
(21) Vetrogon, V. I.; Lukyanenko, N. G.; Schwing-Weill, M.-J.; Arnaud-Neu, F. *Talanta* **1994**, *12*, 2105−2112.
(22) Arnaud-Neu, F.; Barrett, G.; Fanni, S.; Marrs, D.; McGregor, W.; McKervey, M. A.; Schwing-Weill, M.-J.; Vetrogon, V. I.; Wechsler, S. *J. Chem. Soc., Perkin Trans 2* **1995**, 453.

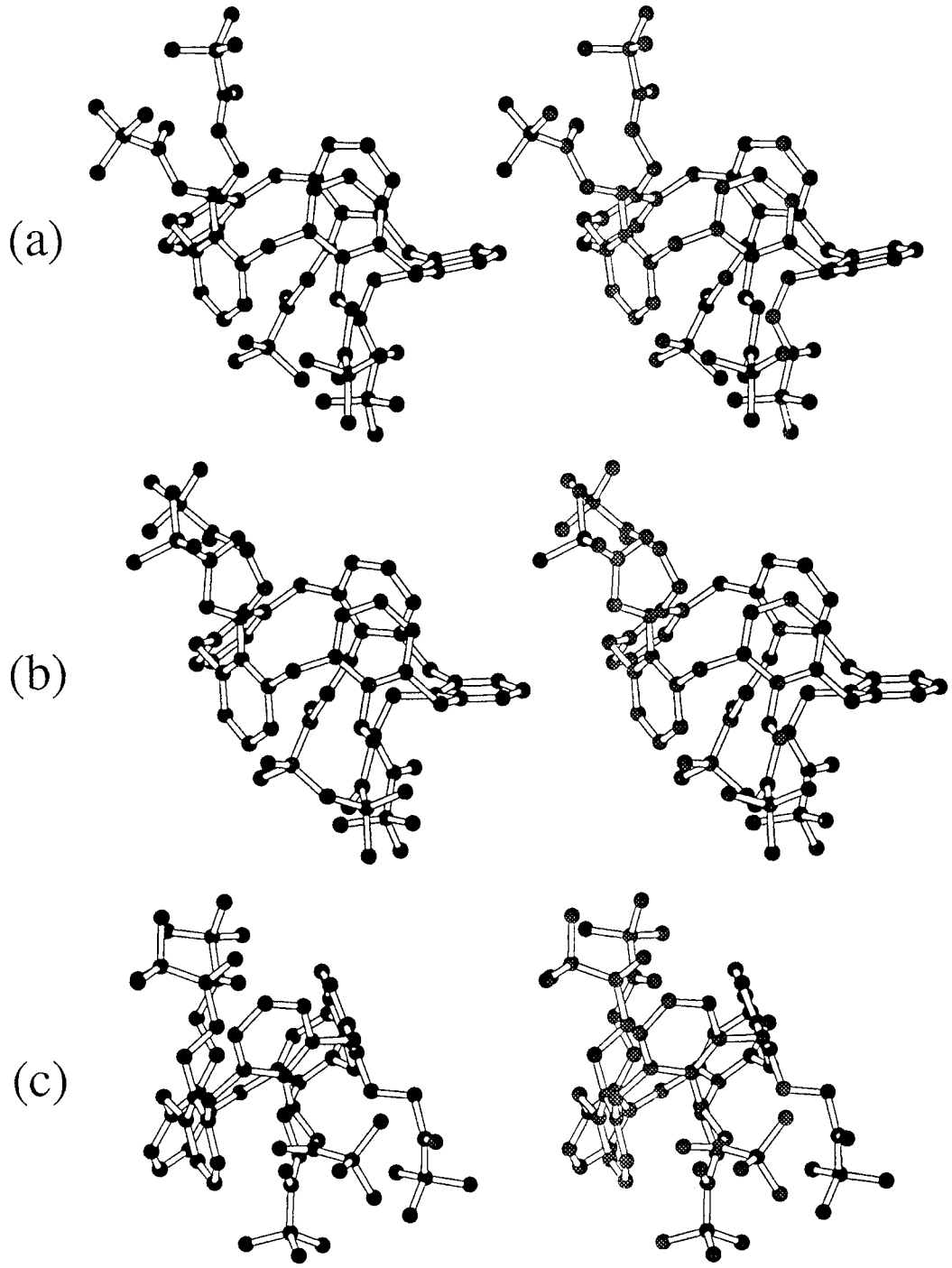

Figure 5. Stereoviews of energy minimized structures of molecule **5** (b and c) and, for comparison, stereoviews (a) of the X-ray structure of **5**.

apparent from comparison of the log β values for **5** with those of **6**, where the latter is consistently the weaker binding ligand. In the pentaester derivatives **12** and **13**, the higher levels of extraction associated with the *tert*-butyl ester **13** are also reflected in stability constants.[14] Obviously, factors other than the lipophilicity of the ligands must be invoked to explain this behavior. As shown by the thermodynamic parameters of complexation of Cs^+ (Table 3), the important increase of stability ($\Delta\log\beta = 2.74$) accompanying the replacement of methyl (compound **6**) by *tert*-butyl groups (compound **5**) is the result of a tremendous increase in the enthalpy change from $-\Delta H_c = 14$ to $-\Delta H_c = 35$ kJ mol^{-1}. The large enthalpy contribution for Cs**5**$^+$ may be related to different factors such as (i) the higher basicity of the carbonyl oxygens due to the presence of *tert*-butyl groups, more donating than methyl groups, (ii) the lower solvation of the ligand due to steric hindrance, and (iii) a better preorganization of the ligand. The small entropy term, even slightly negative as compared to the value for Cs**6**$^+$, would suggest the importance of solvation effects.

On the other hand, the log β values for ketone **1** are also very consistent with the performance of this ketone in extraction, both measurements showing a slight preference for Rb^+. However, comparison between **1** and **6** reveals a slight preference for **1** with respect to the larger cations, except Cs^+, for which thermodynamic parameters are very similar.

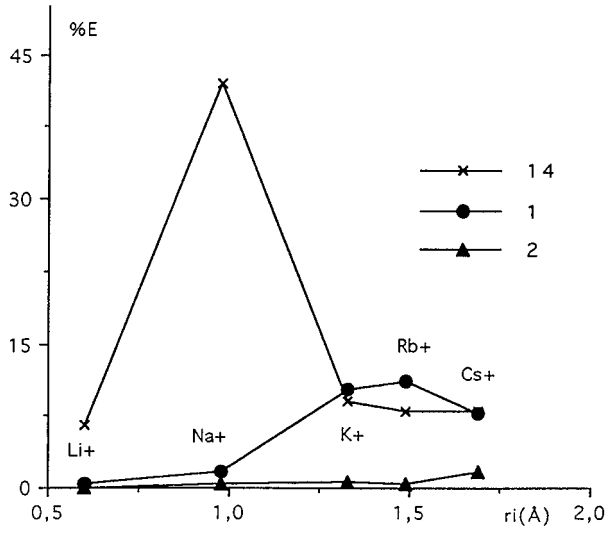

Figure 6. Percentage cation extracted (% *E*) from water into dichloromethane of alkali picrates vs the cation ionic radius: influence of calixarene size in the ketone series.

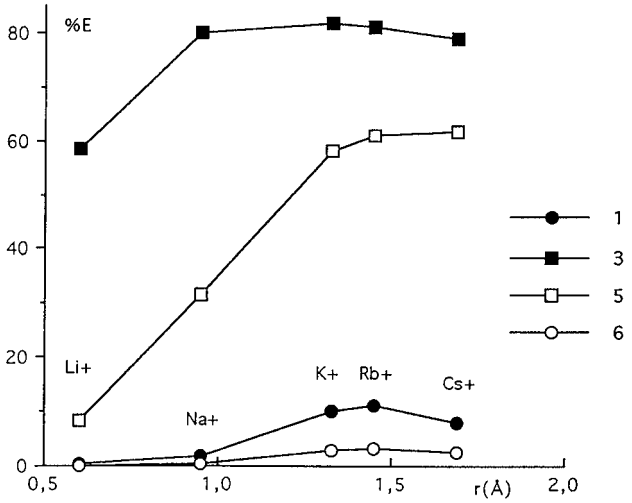

Figure 7. Percentage cation extracted (% *E*) from water into dichloromethane of alkali picrates vs cation ionic radius: substituent effects.

Table 1. Percentage Extraction (%E) of Alkali Picrates into CH_2Cl_2 at 20 °C. Arithmetic Mean of Several Experiments, Standard Deviation on the Mean: $\sigma_{n-1} \leq 1$

compounds	Li^+	Na^+	K^+	Rb^+	Cs^+
5-Me ketone **1**	0.5	1.7	10.2	11.2	7.8
6-Me ketone **2**	0	0.4	0.6	0.5	1.7
5-*tert*-butyl ketone **3**	58.4	80	81.9	81	79
6-*tert*-butyl ketone **4**	0.8	2.0	2.1	2.1	3.1
p-H-5-*tert*-butyl ketone **5**	8.3	31.7	58	61.1	61.8
p-H-5Me ketone **6**	0	0.3	2.8	3.4	2.6
p-H-6Me ketone **7**	0	0	0	0	4.6
5-Et ester[a] **12**	8	33	47	51	51
5-*tert*-butyl ester[a] **13**	25	69	74	72	68
4-Me ketone **14**	6.5	42.3	8.7	7.6	9.6
6-*tert*-butyl ester **15**	0	2.2	2.1	3.3	8.4

[a] Reference 14.

X-ray Crystallographic Analysis of Penta-*tert*-butyl Ketone 3·$Na^+ClO_4^-$. The isolation of good quality crystals of the sodium and rubidium perchlorate complexes of ketone **3** provide an opportunity to probe their solid-state structures by X-ray diffraction. No solid-state structural data exists for calix[5]arene complexes, nor are there data for any metal complex of a calixarene ketone or ester. The structure adopted by the **3**·$NaClO_4$ complex, recrystallized from methanol, is shown in Figure 8.. In the solid state the complex adopts a distorted cone conformation, although to a lesser extent than the free ligand **3**, where one of the aromatic *tert*-butyl groups is oriented toward the hydrophobic upper rim cavity. The tilt angles of the aromatic rings to the bridging methylene mean plane again provides the best structural assessment with angles of (144°: A), (102°: B), (99°: C), (134°: D) and (74°: E). Aside from ring E the remaining aromatic rings all have their *tert*-butyl groups pitched away from the upper rim cavity. The inclination of E again forces adjacent rings A and D to accentuate their outward tilt, although this effect is much more pronounced for ring A than for ring D. Adjacent phenolic O--O separations defining the boundaries of the lower rim calix cage vary between 3.09 Å (O1A−O1E) and 4.63 Å (O1D−O1E) highlighting the concomitant inward/outward distortion. The Na^+ cation is held in a spatial position between the phenolic oxygen plane and the ketonic carbonyl oxygen atoms. This relatively small guest lies off-center from the lower rim calix cage because the oxygen atoms on ring E do not participate in binding and the enclathration cage is instead composed of the remaining ketonic chains. Of these chains, only the phenolic oxygen atom attached to ring A is precluded from electrostatic interaction to Na^+. Its position in the Na^+ coordination cage is instead taken by the oxygen atom of the included methanol solvent molecule with a Na^+--oxygen separation of only 2.33 Å. The Na^+ cation is thus surrounded by an 8 coordinate oxygen cage. The calixarene oxygen--Na^+ separations in this cage vary between 2.28 Å (Na1−O2D) and 2.81 Å (Na1−O1D). The perchlorate counteranion is situated just outside the hydrophilic lower rim cavity and was found to be disordered, unequally, over two sites. Again, as in the free ligand case, some of the *tert*-butyl groups were disordered and where possible were either refined as PART (SHELXL-93)[15] atoms or restrained in a tetrahedral environment.

X-ray Crystallographic Analysis of Penta-*tert*-butyl Ketone 3·$Rb^+ClO_4^-$ Complex. X-ray crystallographic analysis of the $Rb^+ClO_4^-$ complex of **3** was accomplished after recrystallization of the complex from ethanol. The structure of the complex is shown in Figure 9.

In the solid state the structure again adopts a now classical distorted cone conformation with one *tert*-butyl aryl ring inclined to the other upper rim inclination. It is thus apparent from both the Na^+ and Rb^+ complexes of **3** that only small universal conformational changes in the free form of the penta-*tert*-butyl ketone are needed, to effect cationic inclusion. This was presumed on the basis of the high broad extraction capabilities (Table 1) shown by **3**, but is now confirmed through solid-state structural analysis. The tilt angles of the aromatic rings to the macrocyclic ring methylene mean plane again provide the best means of structural definition viz.: (110°: A), (112°: B), (129°: C), (51°: D) and (127°: E). Apart from the sharp inward inclination of D, the remaining aromatic rings all assume outward tilts with their attached *tert*-butyl groups pitched away from the calix cavity by varying degrees. Unlike the previous Na^+ complex case, the inward inclination of ring D in this case is more pronounced, mirroring the tilting extent evidenced in the

Table 2. Log β Values[a] Cations Complexation in Methanol, $T = 25$ °C, $I = 0.1$ mol dm^{-3} Et_4NClO_4 or Et_4NCl

compounds	Li^+	Na^+	K^+	Rb^+	Cs^+
1	<1.5[d]	<1.5[d]	3.34 ± 0.06[d]	3.6 ± 0.2[d]	3.22 ± 0.08[d]
5	<1.5[d]	4.8 ± 0.2[d]	5.67 ± 0.01[e]	5.81 ± 0.08[e]	5.84 ± 0.03[e]
6	<1.5[d]	<1.5[d]	3.1 ± 0.2[d]	3.2 ± 0.3[d]	3.1 ± 0.2[d]
12[b]	1.0	4.4	5.3	5.6	5.5
13[b]	1.5	5.1	6.1	5.8	5.3
14[c]	2.7	5.1	3.1	3.6	3.1

[a] Arithmetic mean of several experiments, standard deviation on the mean: σ_{n-1}. [b] Reference 14. [c] Reference 5. [d] Spectrophotometric determination. [e] Potentiometric determination.

Table 3. Thermodynamic Parameters of Complexation in Methanol of Cs^+ Complexes, $T = 25$ °C

	1	**5**	**6**
$-\Delta G_c$ (kJ mol^{-1})	18.4 ± 0.5	33.3 ± 0.2	18 ± 1
$-\Delta H_c$ (kJ mol^{-1})	15 ± 2	35 ± 0.1	14 ± 2
$T\Delta S_c$ (kJ mol^{-1})	3 ± 2	−2 ± 1	4 ± 3
ΔS_c (J K^{-1} mol^{-1})	10 ± 7	−7 ± 3	13 ± 10

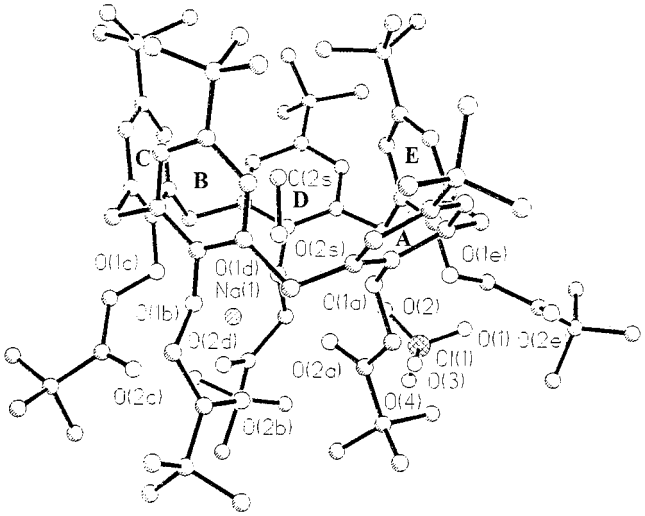

Figure 8. A view of the Na^+ complex of **3** showing the molecular conformation.

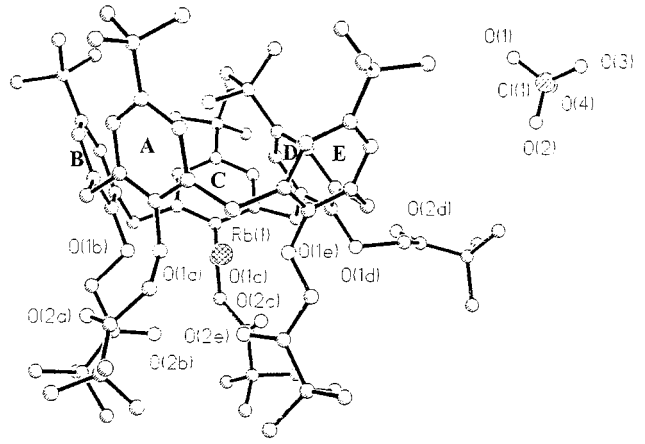

Figure 9. A view of the Rb^+ complex of **3** showing the molecular conformation.

free ligand pentaketone. Presumably the lack of solvent inclusion in the upper rim hydrophobic cavity of the Rb^+ complex permits a similar degree of inward tilt to the free ligand. Again, the inward distortion of ring D on the upper rim forces the adjoining aromatic rings C and E to assume more open orientations reflected in greater outward tilts of 129° for C and 127° for E in relation to rings A and B. Such an effect alleviates the steric interaction between the *tert*-butyl groups on rings C and E to that on ring D. The adjacent phenolic O--O separations on the lower rim boundary vary between 3.25 Å (O1B−O1C) and 4.41 Å (O1D−O1E) and serve to highlight the uneven nature of the aromatic tilting angles. The extremeties of phenolic O--O separation are similar in magnitude to those in the free ligand pentaketone (3.30 and 4.51 Å) implying that very little structural change accompanies Rb^+ inclusion. This feature is further supported by the similarity between the respective aromatic ring tilting angles. The Rb^+ cation is held in a spatial position closer to the phenolic oxygen plane than to the mean plane defined by the ketonic carbonyl oxygen atoms. Unlike the Na^+ complex, the Rb^+ cation occupies a more central position in the lower rim calix cage despite the fact that the oxygen atoms on ring D do not participate in binding. Figure 10 shows an overlay of the two X-ray structures showing the relative position of the Rb^+ and Na^+ cation within the cavity. As was apparent for the Na^+ case, the enclathration cage is composed of, and defined by, the remaining ketonic podands. Of the remaining arms, the carbonyl oxygen atoms (O2) attached to rings A and B are not included in the complexation process. The remaining phenolic and carbonylic oxygen atoms define a 6 coordinate complexation cage for Rb^+. The calixarene--Rb^+ separations in this cage vary between 2.85 and 2.97 Å. The perchlorate counteranion is not disordered in this case and occupies a position beside the upper rim of the macrocycle. Some of the *tert*-butyl groups possessed relatively large thermal parameters and were either refined as disordered atoms partitioned between two sites or tetrahedrally restrained. X-ray diffraction has thus provided an insight into the subtle conformational modifications imposed on the penta-*tert*-butyl ketone by alkali cation encapsulation.

Molecular Mechanics Calculations. Having acquired some structural data from X-ray diffraction and ^{1}H NMR spectra, it became of interest to see if molecular mechanics calculations (MM^+) could provide further insight into these calix[5]arene systems, especially the complexed state. Wipff and co-workers[16] have already demonstrated, in the most sophisticated studies to date, how molecular dynamics can be used to probe the relationship between ligand conformation, cation, and solvent in calix[4]arene amide complexes of alkali cations and Eu^{3+}. For us the first step was to establish that MM calculations could reliably predict structures of the larger and conformationally more heterogeneous calix[5]arenes of lower symmetry.

The energy-minimized MM^+ calculated and X-ray structures of ketone **3** are shown in Figure 11a,b. The MM^+ structure is adequately close to that of the crystal structure; in particular the model reproduces well the inward tilt of one of the aryl rings and, due to the mechanical coupling present in the system, the increased

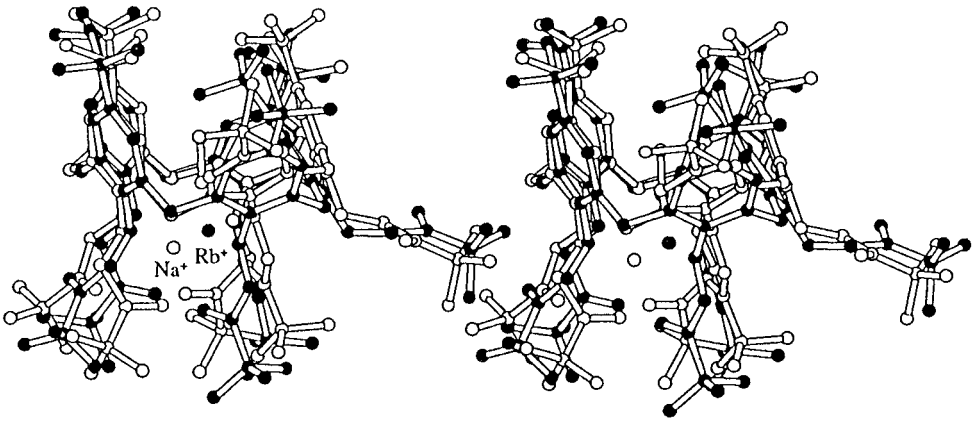

Figure 10. Superimposed stereoviews of the Na^+ and Rb^+ complexes of **3**.

outward tilt of the two adjacent rings. It should be emphasized that the starting geometry for this conformation was built with all aryl rings approximately parallel and upright and that minimization to the tilted structure did not depend on a biased starting geometry. It is clear from closer inspection of the structure that the inward tilt of the unique phenoxy ring must be accompanied by a very substantial movement of its *tert*-butyl group toward the center of the calixarene. In fact, space-filling models show that the remaining four *tert*-butyl groups form a cavity on the lower rim into which the fifth *tert*-butyl group fits exactly.

The Rb^+ complex of **3** has a very similar geometry to that of the metal-free ligand, indicating a high degree of preorganization for complexation. The MM^+ structure of the Rb^+ complex is shown in Figure 11c, along with the actual crystal structure (Figure 11d). It is clear that there is again good agreement between the two structures, despite the very crude nature of the molecular mechanics calculation. The similarity in ligand conformation between the free calixarene **3** and its Rb^+ complex is reproduced and, more impressively, the actual position of the cation in the cavity is also very close in the model structure. It could be argued that this is simply because the cation has found the lowest energy position in a calixarene whose structure the modeling process has been unable to disturb. However, the fact that similar calculations on tetraamide **16** and its K^+ complex (whose X-ray structures are both known)[9] do reproduce the extensive reorganization of the calixarene conformation on complexation argues strongly against this view.

The structure of the Na^+ (MeOH) complex of **3** shows two interesting effects as compared to the Rb^+ complex (Figure 10). The first is that the Na^+ ion lies much farther below the plane of the phenolic oxygens than does the Rb^+ ion, despite the coordination by methanol at the upper rim which would, if anything, be expected to pull the cation even higher. The second is that the unique inward tilting aryl ring is moved to a much more upright position in the Na^+ complex. In addition, the symmetric arrangement of the phenolic rings is lost in the complex with one of those adjacent to the unique ring tilted very far outward and the other tilted significantly less. However, on the basis of the X-ray data alone, it is not possible to tell whether these effects are associated solely with the Na^+ ion or are due to the coordinated solvent molecule. Since the modeling appeared to predict reasonable structures for **3** and its Rb^+ complex, it seemed appropriate to attempt to address these questions by modeling the Na^+ complex of **3** with no methanol in the cavity and then to explore the effect of adding the methanol separately. The energy-minimized structures of the Na^+ complex with and without methanol are shown in Figure 11e,f. In the modeled structure, the complex solvent molecule is in approximately the correct position as is the Na^+ cation. Closer comparison of the modeled and X-ray structures shown in Figure 11f,g shows the model does not exactly reproduce the X-ray structure, because the reorientation of the inward tilting ring is slightly underestimated, as is the additional tilt of the adjacent ring, but the overall fit to the X-ray structure is satisfactory. This gives us some confidence that the modeling procedure is reliable and that it is reasonable to draw conclusions from the model structure for the Na^+ complex in the absence of coordinated solvent. This structure (shown in Figure 11e) retains the overall geometry of the Rb^+ complex, the main difference being that the Na^+ ion lies farther below the phenolic oxygens than does the Rb^+. This implies first that the large difference in the positions of the metal cations observed in the crystal structures (illustrated in Figure 10) is not simply due to the presence of the encapsulated solvent in the Na^+ complex, but a significant part of the difference must arise from a preference of Na^+ for the more electron-rich carbonyl groups over the ether linkages, irrespective of other factors. The position of the Na cation is slightly more central in the model with MeOH bound, so that the solvent inclusion does have a secondary effect on the metal ion position.

Second, changing the metal cation without also adding a solvent molecule does not cause a large change in the orientation of the inward tilting aryl ring in the model structures. However, incorporation of a methanol solvent molecule into the Na^+ complex does force this aryl ring outward so that it adopts the more upright orientation observed in the X-ray structure (Figure 8). The two main differences in the structure of the Rb^+ and Na^+ complexes can thus be attributed to two separate influences: the metal cations will bind at different positions to the undistorted calixarene, while the encapsulated solvent causes the ligand structure to distort.

The fact that the uncomplexed ketone **5** of the *para*-dealkylated calixarene adopts a noncone conformation in the solid state and a mixture of conformations in solution, prompted us to extend the modeling studies to this system. An extensive search of the conformers which this molecule can adopt revealed many local minima on the potential energy hypersurface, similar to the situation

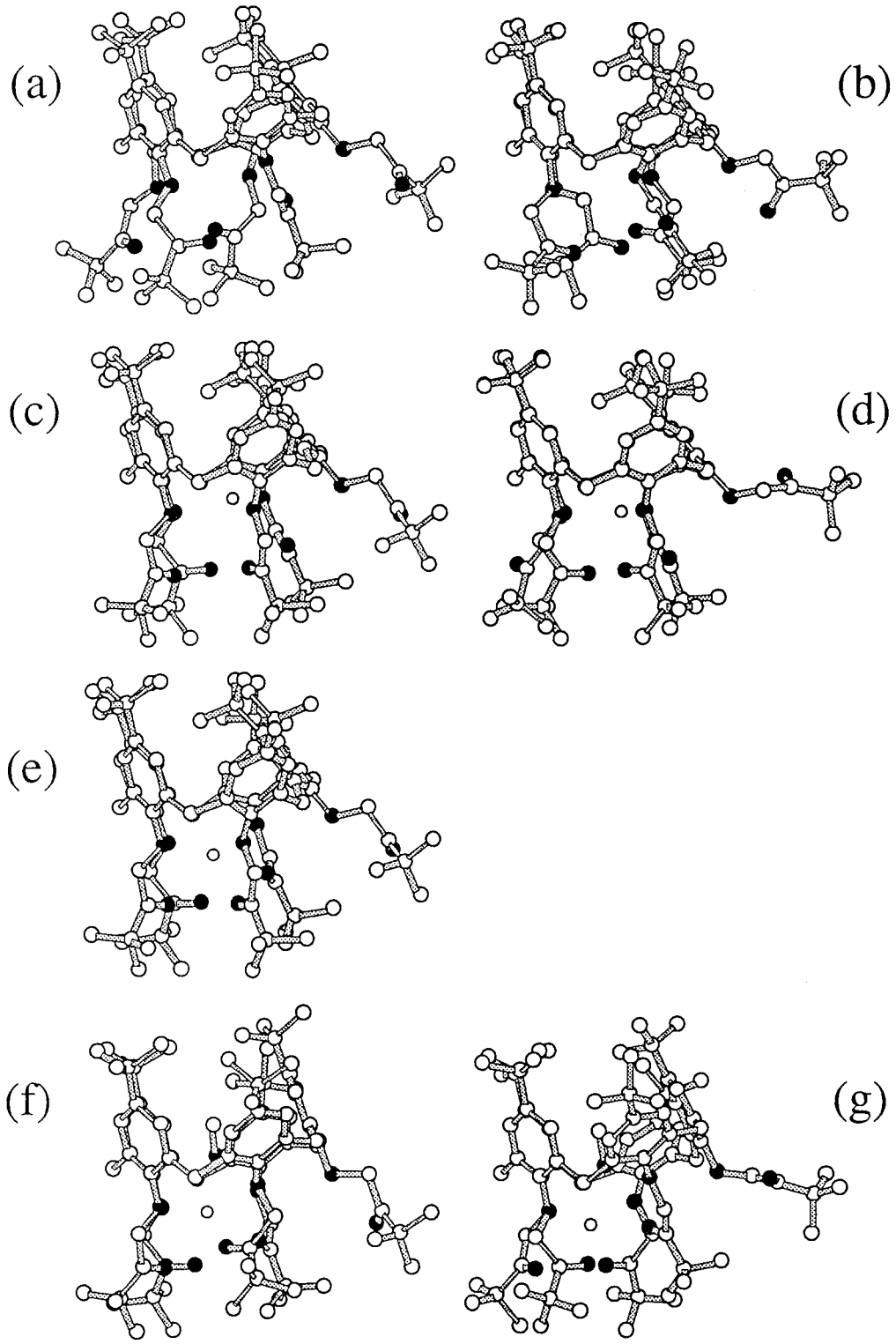

Figure 11. X-ray and energy-minimized structures of molecule **3**. (a) Energy-minimized structure of free ligand. (b) X-ray structure of free ligand. (c) Energy-minimized structure of Rb^+ complex. (d) X-ray structure of Rb^+ complex. (e) Na^+ complex without methanol (energy minimized). (f) Na^+ complex with methanol (energy minimized). (g) Na^+ complex with methanol (X-ray).

encountered by Gutsche in his studies of calix[5]arene ethers and esters.[13] There is evidence from studies of calix[4]arenes that molecular mechanics calculations are not reliable in predicting the lowest energy conformers[17] and there is no a priori reason to suppose that in the conformationally more heterogeneous calix[5]arenes they will prove to be more reliable, except that the increased flexibility of the larger molecules may reduce the interactions between each of the substituted arene rings and allow comparison between relatively unstrained molecules. However, in view of the conformational heterogeneity, it is useful to have some guide to the geometries of the possible conformers and an indication of those which are either very high or reasonably low in energy, to aid interpretation of other data. The structure of the lowest energy conformer resulting from an extensive search of the large number of related structures which can be generated from **5** is shown in Figure 5b, along

with the X-ray structure. In this particular case there is good agreement between both structures. The next lowest lying conformer is the cone, but there are several low energy conformers within a few kcal mol^{-1} of each other; for example, also included in the figure is a second 1,2-partial cone whose energy is approximately 2 kcal mol^{-1} higher than that of the lowest energy form. In solution, conformational averaging similar to that observed for the cone conformer is clearly possible between both 1,2-partial cone structures shown in Figure 5, since their interconversion does not require a full inversion of an aryl ring. This observation emphasizes the main advantage provided by modeling of such systems which is not that the modeling gives a structure very similar to that of the crystal as the lowest energy conformer, but that it can generate a series of low energy structures which, although they cannot be observed crystallographically, may well be important in solution.

Experimental Section

Unless stated otherwise, all reagents were obtained from commercial sources and were used without further purification.

Infrared spectra were obtained using a Perkin-Elmer 983G grating spectrophotometer. Solid samples were dispersed in KBr and recorded as clear pressed disks.

^{1}H NMR spectra were recorded at 300 MHz on a General Electric QC 300 spectrometer and at 500 MHz on a General Electric QE 500 instrument. ^{13}C spectra were recorded at 125 MHz, using a General Electric QE 500 spectrometer. In all cases tetramethylsilane (TMS) was used as an internal standard and chloroform-*d* (deuteriochloroform) as solvent unless otherwise stated. Chemical shifts are expressed in parts per million (ppm or δ) downfield from the standard.

Elemental analyses were determined on a Perkin-Elmer 2400 CHN microanalyzer. Compounds quoted gave elemental analyses to within ±0.5% of theoretical values. Carbon values in microanalysis are frequently low for calixarenes with cavities capable of retaining solvent molecules. In some instances acceptable elemental analysis was only possible if one assumes the inclusion of one or more molecules of solvent.

EI mass spectra were recorded at 70 eV on a VG Autospec instrument using a heated inlet system. Accurate molecular weights were determined by the peak matching method using perfluorokerosene as standard reference. ES mass spectra were recorded on a Fisons VG-Quatro instrument with electrospray inlet. Depending on the molecular weight of the sample, bovine trypsinogen (600−2200 mass range), horse heart myoglobin (700−1800 mass range), or a mix of poly(ethylene glycol)s (300−1400 mass range) were used for calibration purposes.

Crystallographic data for **1** and **3**·$NaClO_4$ were collected at a low temperature on a Siemens P4 four-circle diffractometer. The remaining data sets were collected at rt using a Siemens P3 machine. All the structures were solved by direct methods[23] and refined on F^2 using SHELXL-93.[15]

Analytical TLC was performed on Merck Kieselgel 60_{254} plates. Preparative TLC was carried out with glass plates (20 × 20 cm) coated with Merck Kieselgel $PF_{254+366}$ (21 g in 58 mL of H_2O per plate). Flash chromatography was effected using Merck Kieselgel 60 (230−400 mesh).

Commercial grade solvents were dried and purified by the standard procedures as specified in *Purification of Laboratory Chemicals* (Perrin, D. D.; Armarego, W. L. F.; Perrin, D. R.; Pergamon Press: New York, 1966).

Calix[5]arene (9). A mixture of *p-tert*-butylcalix[5]arene (10.00 g, 12.35 mmol) and finely ground aluminum trichloride (16.47 g, 0.12mol) was stirred vigorously in dry toluene (100 mL) at room temperature for 12 h. Hydrochloric acid (1 N) was then added dropwise to destroy excess aluminum trichloride. Dichloromethane (ca. 3 times the volume of toluene) was added and the solution filtered through Celite. The organic layer was separated and washed in turn with 1 N HCl, brine, and distilled water, each washing being back-extracted with dichloromethane. The organic layer was dried with $MgSO_4$ and concentrated to a pale orange solid. The solid was dissolved in chloroform and subsequently precipitated by the addition of methanol. Recrystallization from toluene afforded calix[5]arene (5.22 g, 80%), mp >275 °C as a cream-colored solid. [Found: C, 79.4; H, 5.4. $C_{35}H_{30}O_5$ requires C, 79.2; H, 5.7%]; ν_{max} (KBr/cm^{-1}) 3300 (OH); δ_H ($CDCl_3$), (300 MHz) 3.85 (10H, bs, ArCH_2Ar), 6.84 (5H, t, J = 7.51 Hz, ArH), 7.21 (10H, d, J = 7.51 Hz, ArH), 8.92 (5H, s, OH).

***p-tert*-Butylcalix[5]arene Penta-*tert*-butyl Ketone (3).** A mixture of *p-tert*-butylcalix[5]arene[18] (4.0 g, 4.94×10^{-3} mol), bromopinacolone (4.42 g, 2.47×10^{-2} mol), potassium iodide (4.10 g, 2.47×10^{-2} mol), anhydrous potassium carbonate (6.35 g, 4.60×10^{-2} mol), and dry acetone (60 mL) was heated under reflux for 24 h. The cooled mixture was filtered through Celite, and the filtrate and dichloromethane washings of the solid residue were combined and washed successively with 3% sulfuric acid (50 mL) and water (2 × 10 mL). The solution was then dried and concentrated at reduced pressure to afford a solid which was taken up in aqueous ethanol and heated under reflux for 3 days. Dichloromethane extraction yielded a solid which on recrystallization from ethanol−dichloromethane furnished **3** (2.83 g, 44%) as white crystals, mp 301−303 °C; ^{1}H NMR ($CDCl_3$, 300 MHz) δ 1.01 (45H, s), 1.22 (45H, s) 3.35 (5H, d, J = 14.5 Hz), 4.73 (5H, d, J = 14.4 Hz), 5.04 (10H, s), 6.87 (10H, s); IR (KBr) λ_{max} 1729/, 1699. Anal. Calcd for $C_{85}H_{120}O_{10}$·H_2O; C, 77.30; H, 9.30. Found: C, 77.40; H, 9.30; MS (ES^+) *m/e*: 1319.7 (M + H + H_2O)$^+$, 1323.5 (M + Na)$^+$, 1324.3 (M + H + Na). $C_{85}H_{120}O_{10}$ requires M^+ 1300.9.

***p-tert*-Butylcalix[5]arene Pentamethyl Ketone (1).** A mixture of *p-tert*-butylcalix[5]arene (5.0 g, 6.17×10^{-3} mol), sodium iodide (8.67 g, 5.79×10^{-2} mol), chloroacetone (5.35 g, 5.79×10^{-2} mol), and potassium carbonate (8.00 g, 5.79×10^{-2} mol) in dry acetone (300 mL) was heated under reflux for 12 h. The cooled mixture was filtered through Celite, and the filtrate and dichloromethane washings of the solid residue were combined and concentrated at reduced pressure to afford an oil. The crude product was suspended in water and stirred at 60 °C for 2 h. Dichloromethane extraction yielded a solid which was recrystallized from ethanol−dichloromethane to afford **1** (4.31 g, 64%), as a white solid, mp 244−246 °C; ^{1}H NMR ($CDCl_3$, 500 MHz, −10 °C) δ 0.75 (3H, s), 1.00−1.09 (6H, bs), 1.15 (18H, s), 1.33 (18H, s), 1.44 (9H, s), 2.11 (6H, s), 3.29 (2H, d, J = 13.6 Hz), 3.34 (1H, d, J = 14.0 Hz), 3.81 (2H, d, J = 14.7 Hz), 4.01 (2H, d, J = 14.7 Hz,), 4.13 (1H, d, J = 12.9 Hz), 4.16 (2H, d, J = 16.5 Hz), 4.17 (2H, s), 4.21 (2H, d, J = 13.6 Hz), 4.22 (4H, s), 4.53 (2H, d, J = 16.5 Hz), 7.10 (2H, d, J = 1.8 Hz), 7.13 (2H, d, J = 1.1 Hz), 7.19 (2H, s), 7.37 (2H, s), 7.58 (2H, s); δ_c ($CDCL_3$) (−10 °C) 25.83, 26.04, 27.74, 30.96, 31.06, 31.17, 31.22, 31.33, 31.39, 31.49, 34.08, 34.22, 76.83, 76.89, 77.10, 125.76, 126.17, 126.54, 126.89, 127.23, 127.66, 127.70, 127.73, 131.65, 132.79, 133.16, 146.09, 146.49, 146.78, 150.74, 151.65, 204.41, 206.33, 210.12; IR (KBr) λ_{max} 1738, 1715 (C═O). Anal. Calcd for $C_{70}H_{90}O_{10}$: C, 77.00; H, 8.30. Found: C, 76.70; H, 8.30: MS (ES^+) *m/e*: 1091.5 (M + H)$^+$, 1109.6 (M + H + H_2O)$^+$, 1113.5 (M + Na)$^+$. $C_{70}H_{90}O_{10}$ requires M^+ 1090.6.

Calix[5]arene Penta *tert*-Butyl Ketone (5). Treatment of calix[5]arene with bromopinacolone in the presence of potassium iodide and potassium carbonate exactly as described above for *tert*-butyl ketone **3** afforded ketone **5** (53%), mp 210−212 °C (from ethanol−dichloromethane); ^{1}H NMR ($CDCl_3$, 300 MHz) δ (cone isomer **5a**) 1.17 (45H, s) 3.31−3.40 (5H, d, J = 14.5 Hz), 4.67 (5H, d, J = 14.5 Hz), 4.87 (10H, s), 6.73 (15H, m); δ (1,2-alternate isomer **5b**) 1.09 (9H, s), 1.12 (18H, s), 1.22 (18H, s), 3.34 (1H, d, J = 14.4 Hz), 3.36 (2H, d, J = 16.6 Hz), 3.85 (2H, d, J = 16.9 Hz), 3.89 (4H, m), 4.42 (1H, d, J = 14.4 Hz), 4.50 (2H, s), 4.51 (2H, d, J = 16.7 Hz), 4.74 (4H, m), 4.77 (2H, d, J = 16.7 Hz), 6.10 (2H, d, J = 7.3 Hz), 6.64 (2H, m), 6.82 (2H, d, J = 7.6 Hz), 6.94 (2H, m), 7.08 (2H, d, J = 7.4 Hz), 7.24 (2H, m) 7.44 (2H, m), 7.54 (1H, t, J = 6.2 Hz); λ_{max} (KBr) 1723 (C═O). Anal. Calcd for $C_{65}H_{80}O_{10}$: C, 76.40; H,

7.90. Found: C. 76.20; H, 8.00: MS (ES^+) *m/e*: 1021.4 ($M + H)^+$, 1039.3 ($M + H + H_2O)^+$, 1059.4 ($M + H)^+$. $C_{65}H_{80}O_{10}$ requires M^+ 1020.56.

Calix[5]arene Pentamethyl Ketone (6). Treatment of calix[5]arene with chloroacetone in the presence of potassium iodide and potassium carbonate exactly as described above for pentamethyl ketone (**1**) afforded **6** (73%) as white crystals, mp 223−225 °C (from ethanol−dichloromethane); ^{1}H NMR ($CDCl_3$, 500 MHz, −10 °C) δ 0.56 (3H, s), 1.43 (6H, bs), 2.14 (6H, s), 3.33 (2H, d, J = 14.3 Hz), 3.40 (1H, d, J = 14.3 Hz), 3.79 (2H, d, J = 14.0 Hz), 3.98 (2H, d, J = 14.3 Hz), 4.04 (4H, m), 4.12 (3H, d, J = 14.Hz, and d, J = 14.3 Hz), 4.20 (2H, d, J = 16.7 Hz), 4.23 (2H, s), 4.53 (2H, d, J = 16.7 Hz), 6.77−6.83 (4H, m), 7.07 (2H, t, J = 7.5 Hz), 7.15−7.29 (5H, m), 7.33 (2H, d, J = 7.5 Hz), 7.57 (2H, d, J = 7.0 Hz); δc ($CDCl_3$) (−10 °C) 25.27, 25.64, 25.95, 26.95, 28.82, 36.71, 76.41, 77.14, 77.20, 124.19, 124.56, 124.93, 128.20, 130.01, 130.51, 130.74, 131.49, 132.96, 133.11, 133.34, 133.59, 153.53, 153.63, 153.74, 203.65, 205.37, 209.53 (C=0); IR λ_{max} (KBr) 1744, 1723 (C=O). Anal. Calcd for $C_{50}H_{50}O_{10}$: C, 74.00; H, 6.20. Found: C, 73.5; H, 6.00; MS (ES^+) *m/e*: 811.4 ($M + H)^+$, 833.4 ($M + Na)^+$, 849.3 ($M + K)^+$. $C_{50}H_{50}O_{10}$ requires M^+ 810.33.

***p-tert*-Butylcalix[6]arene Hexamethyl Ketone (2).** Treatment of *p-tert*-butylcalix[6]arene[19] with chloroacetone, potassium iodide, and potassium carbonate exactly as described above for pentamethyl ketone **1** afforded hexamethyl ketone − (58%), as a colorless solid, mp 237−240 °C (ethanol−dichloromethane); ^{1}H NMR ($CDCl_3$, 300 MHz) δ 1.17 (54H, s), 1.70−1.91 (18H, bs), 3.40−4.20 (24H, br), 7.05 (12H, bs); 1R (KBr) λ_{max} 1735 (C=O). Anal. Calcd for $C_{84}H_{108}O_{12}$: C, 76.44; H, 8.34. Found: C, 77.08; H, 8.25.

***p-tert*-Butylcalix[6]arene Hexa-*tert*-butyl Ketone (4).** Treatment of *p-tert*-butylcalix[6]arene with bromopinacolone, potassium iodide, and potassium carbonate exactly as described above for penta *tert*-butyl ketone **3** afforded hexaketone (70%) as a colorless solid, mp 301−304 °C; ^{1}H NMR ($CDCl_3$, 500 MHz) δ 0.90−1.40 (108H, m), 3.30−3.70 (12H, m), 4.20−4.50 (6H, m), 4.60−5.00 (6H, m), 6.60−7.40 (12H, m); IR (KBr) λ_{max} 1728 (C=O). Anal. Calcd for $C_{102}H_{144}O_{12}\cdot 2H_2O$: C, 76.60; H, 9.01. Found: C, 76.90; H, 8.84.

Calix[6]arene Hexamethyl Ketone (7). Treatment of calix[6]arene with chloroacetone, potassium iodide, and potassium carbonate as described above for hexamethyl ketone afforded hexamethyl ketone as a colorless solid (68%), mp ∼285 °C dec; ^{1}H NMR ($CDCl_3$, 300 MHz) δ 1.80 (18H, bs), 3.90 (12H, bs), 4.18 (12H, bs), 6.90 (36H, t); IR (KBr) λ_{max} 1733 (C=O). Anal. Calcd for $C_{60}H_{60}O_{12}$: C, 74.09; H, 6.17. Found: C, 74.36; H, 6.15.

Picrate Extraction Measurements. Picrate extraction experiments were performed following Pedersen's procedure:[20] 5 mL of a 2.5×10^{-4} M aqueous picrate solution and 5 mL of a 2.5×10^{-4} M solution of calixarene in dichloromethane were agitated in a stoppered glass tube with a mechanical shaker for 2 min and then magnetically stirred in a thermostated water-bath for a minimum of 30 min. In the case of the *p-tert*-butyl calix[5]arene penta *tert*-butyl ketone (**3**), 3 days of stirring were necessary to reach the extraction equilibrium. The solutions were then left standing for 30 min for phase separation, and the concentration of picrate remaining in the aqueous phase was determined spectrophotometrically. Experimental details as well as the preparation of alkali picrates have been previously described.[10] The results, expressed as the percentage (% E) of cation extracted are given in Table 1.

Thermodynamic Parameter Measurements. The stability constants β, β being the concentration ratio $[ML^+]/[M^+][L]$ (with M^+ = cation and L = ligand), have been determined in methanol (Carlo Erba p.a.) by UV absorption spectrophotometry or by potentiometry. The spectrophotometric method consisted of adding increasing amounts of the metal salt solution into 2 mL of ligand solution (C_L ca. 2.5×10^4 mol dm^{-3}) directly in the spectrophotometric cell (1 cm path length), after the absence of any slow complexation kinetics had been checked. Compound **3** was not soluble enough for a spectrophotometric study in methanol. Attempts in acetonitrile were also unsuccessful. The potentiometric measurements were performed in the case of K^+, Rb^+, and Cs^+ which form very strong complexes with ligand **5**. The method, based on the competition with Ag^+ as auxiliary cation, has been described in detail elsewhere.[10] log β value found for the Ag**5**$^+$ complex and used in the calculations was 5.10 ± 0.05. The stability constants derived from both types of measurements (Table 2) were refined by the program Sirko.[21]

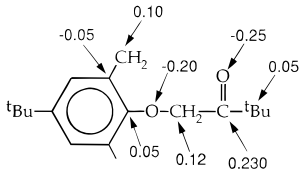

Figure 12. Partial charges used in the MM^+ calculation of the structures of Na**3**$^+$ and Rb**3**$^+$.

The ionic strength of the solutions was maintained at 0.01 mol dm^{-3} by use of Et_4NCl and Et_4NClO_4, for the spectrophotometric and potentiometric measurements, respectively. Et_4NCl was recrystallized twice from acetone, Et_4NClO_4 was washed with acetone before being recrystallized twice from water. Both salts were dried under vacuum for 24 h.

The metallic salts used were the following chlorides: LiCl (Fluka, puriss.), NaCl (Prolabo, Normapur), KCl (Merck, p.a., Fluka, puriss.), and CsCl (Merck, p.a.), the following perchlorates: $AgClO_4$ (Fluka, puriss.), $KClO_4$ (Prolabo, Normapur), RbCl (Sigma), and cesium nitrate ($CsNO_3$) (Fluka, purum).

The enthalpies of complexation ΔH_c of cesium complexes have been determined in the same solvent using an isoperibol titration calorimeter (Tronac 450, Orem, UT). The experimental details have been previously described.[21] The ligand concentrations were in the range 5×10^{-4} 10^{-3} mol dm^{-3}. ΔH_c values were refined by program Sirko,[21] the values of log β determined by spectrophotometry or potentiometry being set as constant. The entropies of complexation ΔS_c were derived from the following equation: $\Delta G_c = \Delta H_c - T\Delta S_c$, knowing $\Delta G_c = -RT \ln \beta$ (Table 3).

Molecular Mechanics Procedures. Calculations were performed using the MM^+ method implemented within the "Hyperchem" molecular modeling package.[25] This all-atom force field is essentially an extended version of MM2.[26] The metal-free structures were minimized using dipole−dipole interactions. The complexes were "built" by inserting the appropriate metal cation approximately in the vicinity of the pendent arms of the calixarene. The metal was fixed in this position during the minimization while the calixarene structure was allowed to relax around it. Electrostatic interactions were explicitly included in the standard way. Partial charges for the calixarene were estimated from a semiempirical (AM1) calculation on a single fragment, i.e., one aryl subunit, of the pentamer. These charges were not scaled in any way and were directly transferred, after some rounding off, and grouping of adjacent charges, to the complex. The partial charges are shown in Figure 12. In the case of structures which included solvent, the solvent molecule was introduced deliberately rotated 90° to its orientation in the X-ray structure, so as to prevent as far as possible an unconscious bias in positioning the molecule near to its known position in the X-ray picture. No extensive conformational searches of the pendent ketone arms were carried out since the large degree of approximation in the model did not justify investigation of such fine detail. The starting structures for all the cation complexes were therefore based on the same model metal-free calixarene.

(23) Sheldrick, G. M. SHELXS 86. *Acta Crystallogr., Sect A* **1990**, *46*, 467.

(24) McKervey, M. A.. Schwing-Weill, M.-J.; Arnaud-Neu, F. In *Comprehensive Supramolecular Chemistry*; Vogel, G. W., Vol. Ed.; Pergamon: New York, 1996; Vol. 1, p 537.

(25) Hyperchem is available from Hypercube Inc., 419 Philips Street, Waterloo, Ontario, N2L 3X2, Canada.

(26) Allinger, N. L. *J. Am. Chem. Soc.* **1977**, *99*, 8127.

More extensive calculations were carried out on the metal-free dealkylated complex **5**. In this case we attempted to build a complete set of the various conformers possible for this sterically less demanding calix[5]arene by using as the initial geometry the cone conformer and then systematically inverting the aryl rings around the cavity. We found that because of the large number of possible conformers more than one starting geometry was needed to generate a closed set of conformers. For example, three starting geometries for the partial cone conformer were used, and these corresponded either to inversion of the inward tilting aryl ring or one of the two adjacent rings or one of the pair opposite. Energy minimization of these structures was followed by a cross-checking procedure where a new set of starting structures was generated by reinversion of the aryl rings, i.e., the partial cone was also built from an energy minimized 1,2-alternate conformer. Energy minimzation of this new set of conformers generated structures which could be compared with those from the first build/minimization cycle. In many cases several structures relaxed to a clearly distinguishable single conformer with a characteristic aryl ring conformation, although the orientation of the alkyl chains were different in each of the relaxed structures. In such cases the lowest energy conformer was chosen. To fully sample the potential energy hypersurface it would be necessary to carry out a full conformational search of each of the alkyl chain conformations within the same aryl ring geometry. However, the number of starting geometries rapidly becomes prohibitive; for example, a set of structures where each of the five unique ketonic carbonyls is allowed only to point inward (toward the core) or outward has $2^5 = 32$ members, if four approximately perpendicular orientations are required the number rises to $4^5 = 1024$.

Supporting Information Available: Tables 1-24 (summary of crystal data and structure refinement, atomic coordinates, bond lengths and angles, anisotropic displacement parameters, and hydrogen coordinates for compounds **1**, **3**, **3**·$NaClO_4$, **3**·$RbCl0_4$ and **5**) (51 pages). This material is contained in libraries on microfiche, immediately follows this article in the microfilm version of the journal, and can be ordered from the ACS; see any current masthead for ordering information.

JO9713114